

Supplementary Information

Interfacing hard and living matter: plasma-assembled proteins on inorganic functional materials for enhanced coupling to cells and tissue

U. Allenstein, F. Szillat, A. Weidt, M. Zink and S. G. Mayr,

Film characterization

PPLL films were characterized with FTIR, XPS, SEM and scratch test measurements.

FTIR measurements: We carried out FTIR measurements with a spectrometer IFS 55 from Bruker Corporation. Unmodified L-lysine and PAF treated L-lysine coatings were investigated in grazing incidence reflection mode. Exemplary spectra for plasma assisted functionalization of gold coated Si are depicted in Figure S1. The substrate was chosen to achieve an adequate reflectivity that could not be provided by the rougher Fe-Pd substrates. By choosing a nobler metal, we ensure transferability of our results, while additionally demonstrating the generalizability of our approach beyond Fe-Pd.

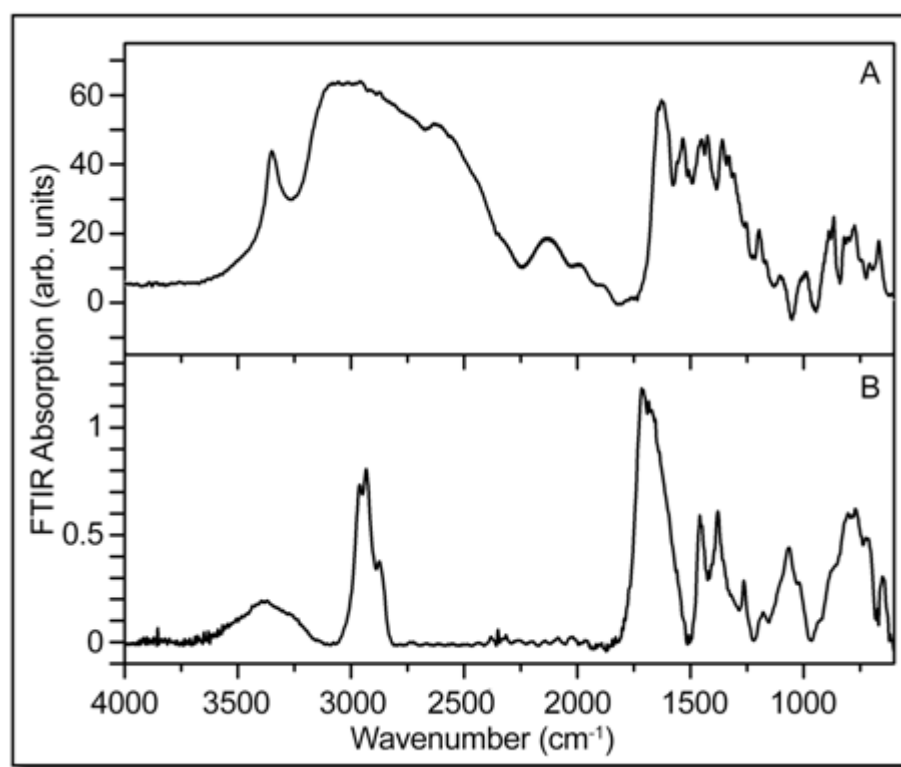


Fig. S1 FTIR spectra of (A) an unmodified L-lysine coating and (B) a representative plasma L-lysine coating on gold coated silicon averaged over 512 subsequent measurements.

XPS Analysis: To verify that the films are closed and to determine the remaining nitrogen content in plasma modified L-lysine, XPS measurements were performed with an Axis Ultra DLD from Kratos Analytical Ltd. Table S2 gives the results for a continuous plasma modified L-lysine on gold coated silicon substrates. The presence of gold could not be detected, which confirms that the polymer films are closed.

Peak	Relative content (at%)
N(1s)	4.2
O(1s)	14.0
C(1s)	81.8

Table S2. Composition of poly-L-lysine coatings resulting from PAF on gold. The absence of a signal originating from the gold substrate shows the closed character of the film.

SEM Imaging: SEM images for visualizing surface structures were obtained with an environmental SEM (Quanta 250, FEI Company) in high vacuum mode at an acceleration voltage of 5 kV.

Scratch tests: Crosslinking of the films was estimated with indentation measurement on an UNAT (universal nano-mechanical tester by ASMEC), where 50 μm long scratches were inflicted on the samples. The spherical indenter with 5 μm radius was pushed to the surface with normal forces between 3 to 120 mN (upper limit of the indenter) and then pulled in lateral direction. The forces to scratch the film were measured and integrated over the scratch length to obtain the work required for film deformation. Results were averaged over 20 scratches.

Density functional theory (DFT) calculations

In addition to the experimental section of the article, further details on the DFT¹ calculations will be given in the following. In general we chose to employ a plane wave code² to be able to calculate energies of fully periodic, partially periodic (i.e. with surface), as well as non-periodic structures consistently. To treat surfaces and non-periodic structures, a supercell approach was chosen (as usual), where sufficiently “vacuum” was inserted into the non-periodic directions to yield results independent of cell dimensions into these directions within the structural convergence limit (see below). Fe₇Pd₃ ferromagnetic shape memory alloys experimentally reside in the disordered face-centered-tetragonal (fct) martensitic phase with a c/a-ratio of 0.946 at physiological conditions, as measured recently with X-ray diffraction and atomic force microscopy for freestanding thin films.³ Due to the very limited amount of atoms feasible in state-of-the-art DFT calculations, i) treatment of disorder and ii) presence of surfaces pose additional challenges. Bearing in mind that ionic relaxations are expected to be of high relevance within the present scope^{4,5} and having to compromise feasible system size vs. exact composition, we chose a 128 atom Fe_{68.75}Pd_{31.25} supercell composed of 2x2x1 special-quasirandom-structures (SQS) supercells^{6,7} of 32 atoms each - with the surface directed in the $\pm z$ directions. Due to the very limited film thickness and the resulting huge surface the volume ratio, surface stress effects shift the phase diagram in favor for a compressed fcc phase⁵ – instead of the experimental fct phase. As this is an artifact of the small simulated system size, the in-plane box dimensions were chosen to obtain the desired fct phase with c/a = 0.946 and fixed.

The starting coordinates for L-lysine were downloaded from the PUBCHEM database,⁸ while fragments and compounds with Fe and Pd were generated from it by removing / adding atoms in the anticipated distance, respectively.

DFT calculations employed ultrasoft pseudopotentials based on the atomic reference configurations 1s¹, [He] 2s²2p², [He] 2s²2p³, [He] 2s²2p⁴, [Ar] 3d⁷4s¹, [Kr] 4d⁹5s¹ for H, C, N, O, Fe and Pd, respectively,⁹ while cutoffs for energy and augmentation charges were chosen at least 476.2 eV and 4762 eV, respectively (higher values were employed for small molecule fractions, if necessary due to convergence tests), using 4x4x1 (in one case up to 8x8x1 to prove convergence) and Γ -only k-point grids for thin film geometries and single molecules, respectively. The electronic ground state is determined self-consistently with the Davidson iterative diagonalization scheme,² employing Methfessel-Paxton smearing¹⁰ (0.2 eV and 0.014 eV for systems involving Fe-Pd films and single molecules, respectively) and a convergence threshold better than 10⁻⁶ meV atom⁻¹. Structural relaxation of the ionic degrees of freedom was generally performed under fixed cell geometries using the Broyden-Fletcher-Goldfarb-Shanno (BFGS) scheme² up to an accuracy of 10⁻⁴ meV atom⁻¹. In some rare cases, convergence could not be reached. If “floppy” modes within the ionic configurations proved to be present with energy oscillations less than $k_{\text{B}}T$ ($T = 300$ K), we assumed that they will be thermally activated under physiological conditions as well; in these cases we thus chose the average of their energies for their energetic quantification. Configurations with convergence issues in electronic or structural relaxation were discarded completely as supposedly “unphysical” structures. Within this context it is worth emphasizing, that by employing identical boxes and parameters for L-lysine and its fragments, as well as pure Fe-Pd and Fe-Pd plus L-lysine, we additionally aimed at minimizing errors.

Figure S3 shows exemplary configurations of a binding and non-binding configuration of L-lysine to a Fe-Pd SQS structure. As binding only occurs between the protein and Fe atoms, an unfavorable distribution of Fe atoms at the surface prevents the occurrence of chemical bonds.

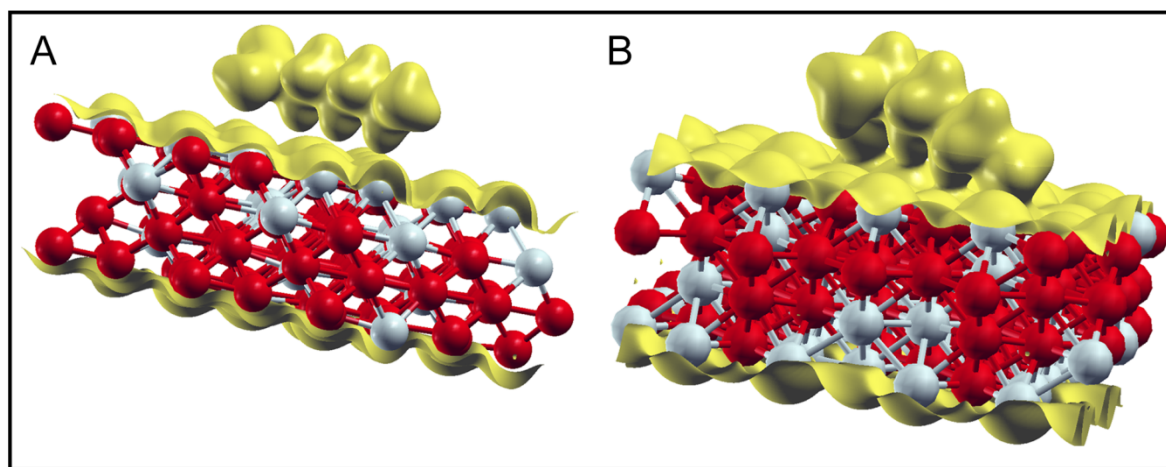


Fig. S3 Special quasi-random Fe-Pd structure (Fe = red, Pd = white) with L-lysine on top. An isosurface corresponding to a charge density of $0.02 \text{ e } \text{\AA}^{-3}$ is visualized in yellow. Opposing to nonbinding configurations (A), binding configurations (B) show non-zero charge between L-lysine and respective iron atoms.

Cell Culture Protocols

The embryonic murine fibroblast cell line NIH/3T3 (ATCC, Manassas, VA) was cultured in Dulbecco's Modified Eagles Medium (PAA, Cambridge), supplemented with 10 % calf serum and 5 ml penicillin/streptomycin antibiotic solution (PS) on 500 ml medium. Cells were incubated at 37 °C in 5 % CO₂ humidified atmosphere. Medium was changed every two to three days.

For proliferation tests, cells on coated Fe-Pd substrates were imaged using a calcein AM – propidium iodide (PI) counterstaining. The calcein solution (life technologies C3099) was applied for one hour. Subsequently, a 5 minute treatment with PI (life technologies P1304MP) followed. The samples were washed with phosphate buffered saline (PBS) before imaging. Besides the investigated PPLL coatings, reference samples for cell adhesion tests were coated with poly-L-lysine from the supplier Sigma-Aldrich (P8920). The solution was diluted with PBS and added to the substrate to achieve a concentration of $2.0 \mu\text{g cm}^{-2}$. After 2 hours incubation at 37 °C, remaining solution was aspirated and cells in the respective growth medium were added.

For imaging, we fluorescently labeled the cells with Millipore's Actin Cytoskeleton and Focal Adhesion Staining Kit (FAK 100), according to the supplier's protocol. It contains TRITC-conjugated Phalloidin to label actin filaments in red and Vinculin combined with FITC-conjugated Goat Anti-Mouse IgG to label focal adhesions in green.

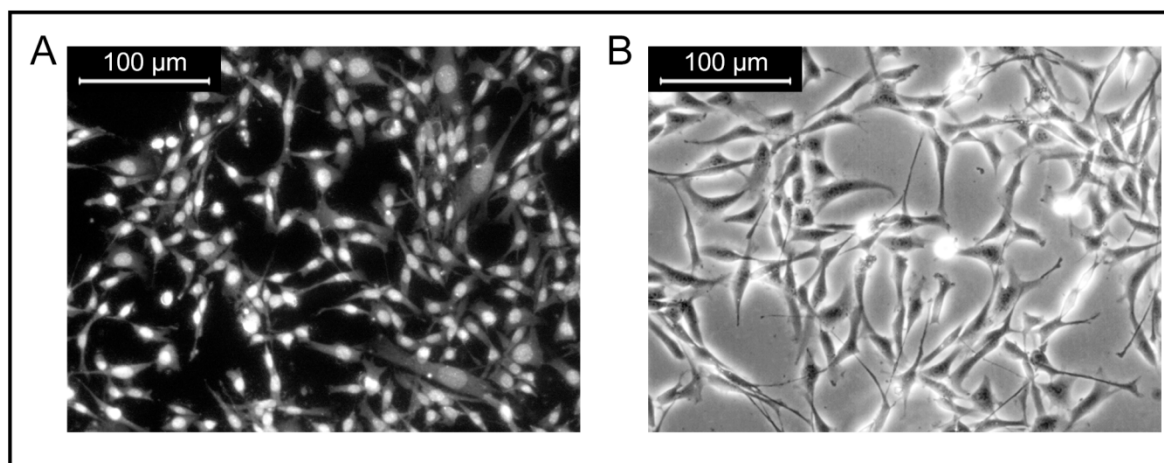


Fig. S4 . Fluorescence micrograph of calcein AM stained NIH/3T3 cells on PPLL coated Fe-Pd (A) and bright field micrograph of NIH/3T3 cells on a polystyrene culture dish (B) both after 4 days of incubation. Higher cell counts in (A) indicate a higher proliferation rate.

- 1 P. Hohenberg and W. Kohn, *Phys. Rev.* 1964, **136**, B864.
- 2 P. Giannozzi, S. Baroni, N. Bonini, M. Calandra, R. Car, C. Cavazzoni, D. Ceresoli, G.L. Chiarotti, M. Cococcioni, I. Dabo, A. Dal Corso, S. de Gironcoli, S. Fabris, G. Fratesi, R. Gebauer, U. Gerstmann, C. Gougoussis, A. Kokalj, M. Lazzeri, L. Martin-Samos, N. Marzari, F. Mauri, R. Mazzarello, S. Paolini, A. Pasquarello, L. Paulatto, C. Sbraccia, S. Scandolo, G. Sclauzero, A.P. Seitsonen, A. Smogunov, P. Umari and R.M. Wentzcovitch, *J. Phys.: Cond. Mat.* 2009, **21**, 395502.
- 3 Y. Ma, A. Setzer, J.W. Gerlach, F. Frost, P. Esquinazi, S.G. Mayr, *Adv. Funct. Mater.* 2012, **22**, 2529.
- 4 M. E. Gruner and P. Entel, *Phys. Rev. B* 2011, **83**, 214415.
- 5 I. Claussen and S.G. Mayr, *New J. Phys.* 2011, 13, 063034, S. G. Mayr, *Phys. Rev. B* 2012, **85**, 014105.
- 6 A. Zunger, S.-H. Wei, L. G. Ferreira and J. E. Bernard, *Phys. Rev. Lett.* 1990, **3**, 353.
- 7 J. von Pezold, A. Dick, M. Friak and J. Neugebauer, *Phys. Rev. B* 2010, **81**, 094203.
- 8 <http://pubchem.ncbi.nlm.nih.gov>, accessed January 14, 2013
- 9 Files H.pbe-rrkjus.UPF, C.pbe-rrkjus.UPF, N.pbe-rrkjus.UPF, O.pbe-rrkjus.UPF, Fe.pbe-nd-rrkjus.UPF, Pd.pbe-rrkjus.UPF, as available at <http://www.pwscf.org>, accessed December 2012.
- 10 M. Methfessel and A.T. Paxton, *Phys. Rev. B* 1989, **40**, 3616